THE JOURNAL OF BIOLOGICAL CHEMISTRY VOL. 284, NO. 27, pp. 18129–18142, July 3, 2009

Identification and Characterization of RBEL1 Subfamily of GTPases in the Ras Superfamily Involved in Cell Growth Regulation*

Received for publication, April 16, 2009 Published, JBC Papers in Press, May 11, 2009, DOI 10.1074/jbc.M109.009597

JoAnne Montalbano, Ki Lui[1], M. Saeed Sheikh, and Ying Huang[2]

From the Department of Pharmacology, State University of New York, Upstate Medical University, Syracuse, New York 13210

Recently, we reported the identification of a novel gene named RBEL1 (Rab-like protein 1) and characterized its two encoded isoforms, RBEL1A and RBEL1B, that function as novel GTPases of Ras superfamily. Here we report the identification of two additional splice variants of RBEL1 that we have named RBEL1C and -D. All four RBEL1 isoforms (A, B, C, and D) have identical N termini harboring the Rab-like GTPase domains but contain variable C termini. Although all isoforms can be detected in both cytoplasm and nucleus, RBEL1A is predominantly cytoplasmic, whereas RBEL1B is mostly nuclear. RBEL1C and -D, by contrast, are evenly distributed between the cytoplasm and nucleus. Furthermore, all four RBEL1 proteins are also capable of associating with cellular membrane. The RBEL1 proteins also exhibit a unique nucleotide-binding potential and, whereas the larger A and B isoforms are mainly GTP-bound, the smaller C and D variants bind to both GTP and GDP. Furthermore, a regulatory region at amino acid position 236–302 immediately adjacent to the GTP-binding domain is important for GTP-binding potential of RBEL1A, because deletion of this region converts RBEL1A from predominantly GTP-bound to GDP-bound. RBEL1 knockdown via RNA interference results in marked cell growth suppression, which is associated with morphological and biochemical features of apoptosis as well as inhibition of extracellular signal-regulated kinase phosphorylation. Taken together, our results indicate that RBEL1 proteins are linked to cell growth and survival and possess unique biochemical, cellular, and functional characteristics and, therefore, appear to form a novel subfamily of GTPases within the Ras superfamily.

The Ras superfamily is known to comprise five structurally distinct subfamilies of small GTPases, including Ras, Rho, Rab, Sar1/Arf, and Ran, and each subfamily of these GTPases possess distinct functions in the regulation of a variety of cellular processes such as cell proliferation, cell differentiation, cytoskeletal organization, protein transport, and trafficking (1–4). The Ras subfamily of GTPases (N-, H-, and K-Ras) function predominantly in relaying signals from receptors at the plasma membrane and modulating cell signaling pathways that regulate cell proliferation, differentiation, and survival (5). Ran GTPase, on other hand, is a key regulator of nucleocytoplasmic transport that regulates protein transport across the nuclear pore complex (6, 7). The Rab subfamily is the largest subfamily among the Ras superfamily and contains more than 60 members. The key functions of the Rab GTPases are to regulate protein exocytic and endocytic pathways and modulate intracellular protein transport/trafficking (8–13).

In general, the Ras superfamily GTPases cycle between an active GTP-bound state and an inactive GDP-bound state. There are five N-terminal motifs involved in the binding and hydrolysis of GTP that are highly conserved among all GTPases: G1 (G*XXXX*GK(S/T)), G2 (T), G3 (D*XX*G), G4 ((N/T)(K/Q)*X*D), and G5 (E*X*SA*X*). Each sequence has particular functions involved in binding nucleotides (GTP or GDP) and facilitating hydrolysis (4, 14, 15). In general, the intrinsic GTPase activity (converting GTP to GDP) and exchange of GDP for GTP are slow processes for these GTPases and thus require regulatory proteins such as GTPase-activating proteins and GDP/GTP exchange factors to facilitate these processes (16–18).

For the last two decades, the Ras superfamily has been a major focus in the cancer field as many of the members are either mutated or dysregulated in cancer. The founding members of the Ras superfamily, H-Ras and K-Ras, were first identified as viral oncogenes (1, 4). Later studies demonstrated that mutations of the Ras proteins (H-, N-, and K-Ras) occur frequently in human cancers, and the mutations identified are mostly clustered within the GTP-binding domains of the proteins thus locking Ras proteins in a GTP-bound configuration. GTP-bound Ras is constitutively active; it constantly activates its effector proteins to transduce cell proliferative signals (1, 4). Unlike Ras subfamily genes, mutations occurring in Rab and Rab-like genes are less common, yet alterations in gene expression of a number of Rab genes have been reported in multiple human malignancies. For example, Rab25 overexpression has been linked to prostate cancer progression (19). Rab2 overexpression has been found in lung adenomas and adenocarcinomas (20). In addition, alterations in Rab gene expression have also been linked to cancer drug resistance. For instance, resistance to the anticancer drug doxorubicin in MCF-7 cells has been linked with reduced expression of Rab6C, and introduction of exogenous Rab6C restores drug sensitivity (21).

* This work was supported, in whole or in part, by National Institutes of Health Grants CA113868 (to Y. H.), DK067271 (to Y. H.), and ES014489 (to M. S. S.).
The nucleotide sequence(s) reported in this paper has been submitted to the GenBank™/EBI Data Bank with accession number(s) GQ169126 and GQ169127.
[1] Supported in part by a DoD Predoctoral Fellowship from the U.S. Department of Defense (Grant BC083017).
[2] To whom correspondence should be addressed: Dept. of Pharmacology, State University of New York, Upstate Medical University, 750 E. Adams St., Syracuse, NY 13210. Tel.: 315-464-8009; Fax: 315-464-9680; E-mail: huangy@upstate.edu.

We have recently reported the identification two novel Ras superfamily GTPases, RBEL1A and RBEL1B (22). RBEL1A and RBEL1B are two splice variants of the *RBEL1* gene and are highly homologous to the Rab and Ran GTPases within their N-terminal GTP-binding domains (22). Our studies show that both RBEL1A and -B predominantly bind to GTP. A single point mutation (T57N) in the GTP-binding domain of RBEL1A and -B abolishes their ability to bind to both GTP and GDP. Both RBEL1A and RBEL1B localize in the nucleus as well as in the cytosol. Whereas RBEL1A is predominantly cytosolic, RBEL1B is primarily nuclear. Interestingly, our studies also suggested that nucleotide (GTP or GDP)-binding could be important for the nuclear distribution of RBEL1B, because the nucleotide binding-deficient mutant form (T57N) of RBEL1B did not reside in the nucleus but rather became largely cytosolic (22).

In our continuous efforts to fully elucidate the function of RBEL1, we have identified two additional splice variants that we have named RBEL1C and RBEL1D. Here we report further characterization of all four RBEL1 splice variants in terms of their GTPase activities, subcellular localizations, regulations, and potential functions. Our results indicate that RBEL1 GTPases, although sharing some common features with other Ras superfamily members, also harbor unique characteristics that are significantly different from other Ras superfamily GTPases. Based on our findings, we suggest that RBEL1 proteins appear to form a novel subfamily of GTPases within the Ras superfamily.

EXPERIMENTAL PROCEDURES

Reagents and Expression Constructs—Anti-HA[3] monoclonal antibodies (HA.11) were from Covance (Berkeley, CA). The β-actin and α-tubulin antibodies were from Sigma. The Lamin B monoclonal antibodies were from Calbiochem. Anti-human RBEL1 antibodies were generated through a commercial source (Pocono Rabbit Farm & Laboratory, Canandensis, PA) as described previously (22).

HA-tagged RBEL1A and RBEL1B were described previously (22). HA-tagged RBEL1A truncations: RBEL1A Δ235, RBEL1A Δ302, RBEL1A Δ361, and RBEL1A Δ624 were generated by amplifying the indicated regions by PCR using full-length RBEL1A as a template and were subsequently subcloned into the pSRαHAS mammalian expression construct. To generate the HA-tagged RBEL1C and RBEL1D constructs, their full-length open reading frames were amplified by RT-PCR from MCF-7 cells and were subcloned into the pSRαHAS expression construct. All vectors were sequenced to confirm correct sequences and reading frames.

PCR Amplification—RT-PCR was performed as we have previously described (23), except the first strand cDNA was synthesized with the Superscript III RT-PCR kit (Invitrogen). Priming regions of the PCR amplification for various RBEL1 splicing variants are illustrated in Fig. 1*A*. For the RBEL1A isoform (primer set A) the sense primer was 5′-CCGATGTGACTGACGAGGATGAG-3′ and the antisense primer was 5′-GTGTTTGCTCTTCTTCTTGGCAGC-3′. For the RBEL1B isoform (primer set B): sense primer, 5′-CATCATCTCTAGGCCGCCACCCT-3′ and antisense primer, 5′-ATGCTGCCTTCGGTCTCGCAG-3′. For cloning of the full-length RBEL1C open reading frame (primer set C1): sense primer, 5′-CCGAGCGGGAAGATGTTTTC-3′ and antisense primer, 5′-GGCTTTGGAAGGGTTTGGAG-3′. For detecting RBEL1C isoform splicing junction (primer set C2): sense primer, 5′-AGTGTGCGTGCTGGGAAACTAC-3′ and antisense primer, 5′-AATCCAGGGGCAAGACAAAGAG-3′. For cloning of the full-length RBEL1D open reading frame (primer set D1): sense primer, 5′-GATGTTTTCCGCCCTGAAGAAG-3′ and antisense primer, 5′-CCCTTGCCAGCAGCCAATC-3′. For detection of RBEL1D splicing junction (primer set D2): sense primer, 5′-CGACATTACCAAGCAGTGGACC-3′ and antisense primer, 5′-TTGCTACACAGGAGACACCTG-3′. For amplification of β-actin cDNA: sense primer, 5′-TCTTTGAGACCTTCAACACCC-3′ and antisense primer, 5′-AGCACTGTGTTGGCGTACAG-3′. To ensure accurate sequences of the RT-PCR products, purified PCR products were subcloned into the pCR2.1 vector using the TA-cloning kit (Invitrogen) followed by DNA sequencing.

RNA Blot Hybridizations—Northern blotting and hybridizations were performed according to standard procedures we previously described (23, 24). To detect RBEL1 isoforms, human RBEL1 cDNA probes recognizing all RBEL1 isoforms (*probe 1*, Fig. 1) or various RBEL1 isoforms (*probes 2* and *3* in Fig. 1*A*) were used. To detect RBEL1C and -D specifically, PCR primers were used to amplify a 387-bp fragment with sequence corresponding to a region unique only to the C and D isoforms (Fig. 1*A*). The primer sequences for probe 2 as the following: sense primer, 5′-TCGTCCTGGTGTCAGAAGAA-3′; antisense primer, 5′-GCAAGACAAAGAGGAAACAG-3′. Probe 3 was also generated by PCR by amplifying a 323-bp region found only in RBEL1D (sense primer, 5′-TGGACCTGCTCGGAGATTG-3′; antisense primer, 5′-TGAACAGCGACCTCGGTGA-3′).

Western Blotting, Immunostaining, and Cell Fractionation—Western blotting and immunostaining were performed as described previously (22, 25). Nuclear and cytosolic fractionations were also prepared as we previously described (22). For membrane fractionation, RKO cells were transiently transfected with HA-tagged RBEL1A, -B, -C, and -D expression constructs. Twenty-four hours later, cells were harvested, resuspended, and homogenized in 400 μl of homogenizing buffer, containing 0.25 M sucrose, 10 mM HEPES (pH = 7.4), 10 mM KCl, 1.5 mM $MgCl_2$, 5 mM EDTA, 5 mM EGTA, 10 mM phenylmethylsulfonyl fluoride, 20 μg/ml leupeptin. Cell lysates were then centrifuged at 100,000 × *g* for 1 h and thus were separated into the supernatant portion (containing cytosolic proteins) and the pellet portion (containing peripheral and integral membrane proteins). The pellet portions were then resuspended in 200 μl of 100 mM Na_2CO_3, pH 11.5, followed by vigorous shaking at 4 °C for 30 min. After that, the homogenates were centrifuged at 240,000 × *g* for 1 h and, again, separated into the supernatants (containing peripheral membrane proteins) and the pellets (containing integral membrane pro-

[3] The abbreviations used are: HA, hemagglutinin; RT, reverse transcription; NAHase, *β-N*-acetylhexosaminidase; shRNA, short hairpin RNA; m.o.i., multiplicity of infection; MTT, 3-(4,5-dimethylthiazol-2-yl)-2,5-diphenyltetrazolium bromide; ERK, extracellular signal-regulated kinase.

teins), which were then dissolved in 100 μl of 1× SDS loading dye. Subsequently, a fraction of RBEL1A, -B, and -C, RBEL1D-R52V (20% total volume), and RBEL1D-WT (40% total volume) was separated by SDS-PAGE electrophoresis and followed by Western blot analysis using antibodies specific to HA tag (Covance, Princeton, NJ), α-tubulin (Sigma), p97 (Fitzgerald, Concord, MA), and calnexin (Stressgen, Ann Arbor, MI) to facilitate the determination of intracellular protein distributions and the purity of each fraction.

β-N-Acetylhexosaminidase Digestion—NAHase digestion was performed per the manufacturer's instructions (New England Biolabs, MA) as we previously described (22). In brief, 293T cells were transiently transfected with either HA-tagged RBEL1A or RBEL1C or RBEL1D expression vectors, and 24 h after transfection cell lysates were prepared. 50 μg of total protein representing cell lysates was incubated in reaction buffer (provided by the vendor) in the presence of NAHase (25 units), and ~24 h following digestion, all samples were analyzed by Western blotting using anti-HA antibodies.

In Vitro GTPase Assay—RBEL1 GTP and GDP binding assay was performed by procedures described in our previous studies (22, 26). In brief, cells were transiently transfected with indicted expression vectors or control vectors and labeled with [^{32}P]orthophosphoric acid (PerkinElmer Life Sciences) as described (22, 26). Following labeling, cells were lysed, and activated charcoal was added to remove excess radioactive phosphorus. Proteins were immunoprecipitated with anti-tag antibodies and bead-bound immunoprecipitants were then eluted, and equal amounts of each immunoprecipitate were spotted and run on a cellulose polyester foil-backed layers plate and exposed to phosphorimaging.

RBEL1 Knockdown—RBEL1-specific shRNA and scrambled shRNA constructs in the pLKO.1 lentiviral vector were designed by The RNA interference Consortium and purchased from Open Biosystems (Huntsville, AL). Lentiviral particles were generated according to the manufacturer's protocol. Briefly, 293T cells were transfected with scramble or RBEL1 shRNA vectors along with the psPAX2 packaging plasmid and pMD2.G envelope plasmid. Media containing virus was harvested 2 and 3 days post-transfection. The viral titer was calculated according the protocol recommended by the RNA interference Consortium and Open Biosystems. Briefly, on Day 1, 5×10^4 HeLa cells were plated in 24-well plates. The following day, cells were infected with 5-fold serial dilutions of the virus in Dulbecco's modified Eagle's medium containing 8 μg/ml Polybrene. Puromycin was added 24 h post-infection. The viral titer was calculated by the number of puromycin-resistant colonies present at the highest dilution multiplied by the dilution factor, which equaled the number of transducing units/ml. A multiplicity of infection (m.o.i.) of 0.3 was used for all experiments. Lentiviral particles were added to Dulbecco's modified Eagle's medium media containing 8 μg/ml Polybrene and then added to cells (RKO, MCF-7, and T47D). For MTT and cell doubling time experiments, lentiviral particle-infected cells were trypsinized 3 days post-infection then plated at equal number and assayed at indicated times. The RBEL1 shRNA targeted sequences are shown below (with an order of sense, loop (underlined), and antisense): RBEL**58**, CCGCCAGTGTTTCTCAGGGATCTCGAGATCCCTGAGAAACACTGGCGG; RBEL**59**, CGGCCTAAAGTACCTTCATAACTCGAGTTATGAAGGTACTTTAGGCCG; RBEL**60**, GCAGTGGACCTTCAATTACATCTCGAGATGTAATTGAAGGTCCACTGC; RBEL**61**, GAAGAATGACTCGGACCTCTTCTCGAGAAGAGGTCCGAGTCATTCTTC; and RBEL**62**, CCAGTCAAGACATCACTCTTTCTCGAGAAAGAGTGATGTCTTGACTGG.

Cell Growth Curves—MCF-7 cells were plated at an equal density and infected with equal doses of lentivirus containing scrambled shRNA or RBEL1-specific shRNAs #58, #61, or #62. One day post-infection, cells were subject to puromycin (5 μg/ml) selection, and the following day, cells were plated at equal density (6.25×10^4 cells/60-mm plate). Cells were trypsinized and counted on days 4, 6, 8, and 10 post-infection.

MTT and Caspase-3 Activity Assay—MTT assays were performed using MTT assay kit (Sigma) according to the supplier's protocol. Briefly, MTT powder was dissolved in Dulbecco's modified Eagle's medium with 10% fetal bovine serum to a final concentration of 1 mg/ml. After 2-h incubation time, media was removed, and the precipitate was dissolved in isopropanol with 0.04 M HCl. Absorbance was read with a Bio-Rad SmartSpec 3100 at 570 nm with background subtraction read at 650 nm. Absorbance was plotted as a percentage of the shRNA scramble control. To measure the caspase-3 activity, RKO cells were incubated with lentiviral constructs carrying either the scrambled shRNA or RBEL1 shRNAs (#59 and #60) in the presence of 8 ng/ml Polybrene overnight, then replaced with fresh growth medium and continued to culture for 4 days. After that, the cells were harvested, and cell lysates were used in caspase 3 assay according to manufacturer's protocol (BD Biosciences Pharmingen). The fluorescent signals were detected by using a Synergy^{TM} HT fluorescence microplate reader (BioTek, Winooski, VT).

RESULTS

Identification and Expression of RBEL1C and RBEL1D—We have recently reported the identification and characterization of two splice variants (RBEL1A and -B) of the *RBEL1* gene (22). Using a computer-based approach, we have now identified two additional RBEL1 splicing variants, which we have named RBEL1C and RBEL1D. Fig. 1 (*A–D*) shows the cDNA and protein sequences, as well as, the genomic and protein structural organization of RBEL1C and RBEL1D. As shown in Fig. 1, both RBEL1C and -D isoforms are much smaller than the RBEL1A and -B variants. RBEL1A is composed of 729 amino acids with a molecular mass of ~80–125 kDa (with protein modification), whereas RBEL1B harbors 520 amino acids with a molecular mass of 62–75 kDa. However, the RBEL1C encodes a protein of 314 amino acids with a predicted molecular mass of ~35 kDa; RBEL1D contains 257 residues with a predicted protein mass of 28 kDa. Both RBEL1C and -D are identical across the first 6 exons, which encode the Rab-like GTPase domain. It is of note that this region is also shared by RBEL1 isoforms A and B (Fig. 1*A*). As for RBEL1C cDNA, exon 7 (7α) is indistinguishable from that of the RBEL1A and -B; but the exon 8 (8β) (the last exon for this protein) is unique and not possessed by other RBEL1 variants. Unlike all other RBEL1 splicing variants,

RBEL1D contains only 7 exons. The exon 7 (7β) of the RBEL1D is much longer than other RBEL1 splicing variants. It harbors a 5′ sequence, which is identical to exon 7α that is shared by A, B, and C and a 3′ sequence, which contains the intron 7 sequence of the RBEL1C plus the exon 8 (8β) sequence of RBEL1C.

Like other Ras superfamily GTPases, each of the RBEL1 proteins harbors five highly conserved GTPase motifs at its N terminus involved in nucleotide binding and hydrolysis (Fig. 1, *B–D*, shown in bold and underlined). Three of RBEL1's GTPase domains deviate from the canonical GTP-binding consensus sequences in the third (D*XX*G(K/Q)→D*XX***D**K), fourth (NK*X*D→N**Y***X*D), and fifth (E*X*SA*X*→E*XS***M***X*) GDP/GTP binding domains. Interestingly, RBEL1C contains a potential "CAA*X*" motif (CSIP) at the very C terminus (Fig. 1, *B* and *C*), which is not shared by any of the other RBEL1 isoforms. The prenylation of C-terminal cysteines is a common post-translational modification for Ras, Rho, and Rab proteins, but it is not a feature of the Ran protein (3, 27). Even though computer-based programs predict a weak propensity for prenylation of RBEL1C at its C-terminal cysteine residue, whether RBEL1C protein can be prenylated is an issue that remains to be determined. Among the RBEL1 proteins, RBEL1D is the smallest isoform; it possesses only 22 amino acids in addition to the shared GTPase domain sequence (Fig. 1, *B* and *D*). Furthermore, both RBEL1C and -D isoforms do not contain the proline-rich regions present in the RBEL1A and -B variants or the nuclear localization signal, which is possessed by RBEL1A.

Our previous studies have shown that RBEL1A mRNA expression is highly abundant and easily detected by Northern blotting; whereas RBEL1B transcript expressed at very low levels can be detected only by RT-PCR but not by Northern blotting. Similarly, Western blot analyses only detect the RBEL1A but not the B isoform (22). To deter-

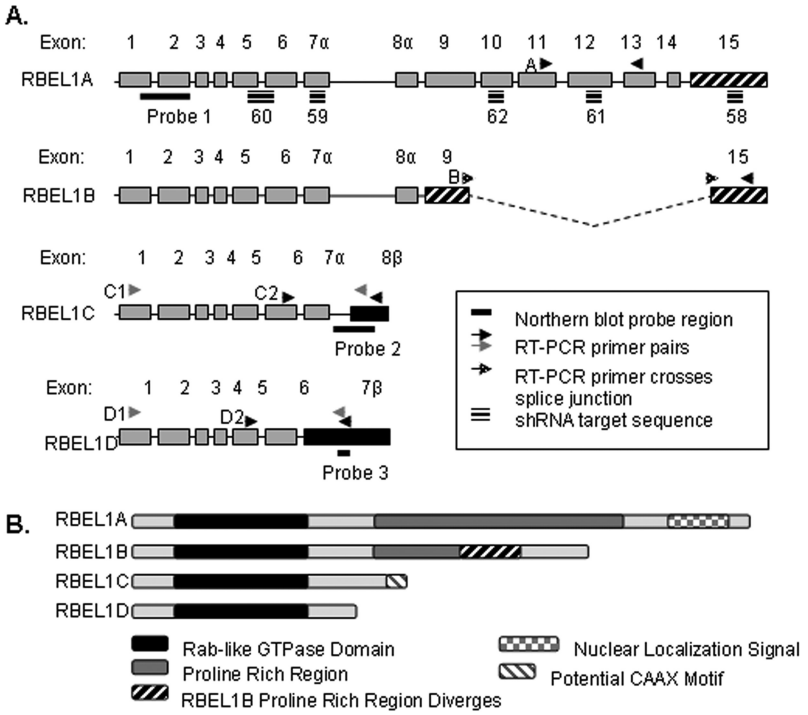

C. RBEL1C

```
ATGTTTTCCGCCCTGAAGAAGCTGGTGGGGTCGGACCAGGCCCCGGGCCGGGACAAGAACATCCCCGCCGGGCTGCAGTCCATGAACCAGGCGTTGCAGA
M F S A L K K L V G S D Q A P G R D K N I P A G L Q S M N Q A L Q

GGCGCTTCGCCAAGGGGGTGCAGTACAACATGAAGATAGTGATCCGGGGAGACAGGAACACGGGCAAGACAGCGCTGTGGCACCGCCTGCAGGGCCGGCC
R R F A K G V Q Y N M K I V I R G D R N T G K T A L W H R L Q G R P

GTTCGTGGAGGAGTACATCCCCACACAGGAGATCCAGGTCACCAGCATCCACTGGAGCTACAAGACCACGGATGACATCGTGAAGGTTGAAGTCTGGGAT
F V E E Y I P T Q E I Q V T S I H W S Y K T T D D I V K V E V W D

GTAGTAGACAAAGGAAAATGCAAAAAGCGAGGCGACGGCTTAAAGATGGAGAACGACCCCCAGGAGGCGGAGTCTGAAATGGCCCTGGATGCTGAGTTCC
V V D K G K C K K R G D G L K M E N D P Q E A E S E M A L D A E F

TGGACGTGTACAAGAACTGCAACGGGGTGGTCATGATGTTCGACATTACCAAGCAGTGGACCTTCAATTACATTCTCCGGGAGCTTCCAAAAGTGCCCAC
L D V Y K N C N G V V M M F D I T K Q W T F N Y I L R E L P K V P T

CCACGTGCCAGTGTGCGTGCTGGGAAACTACCGGGACATGGGCGAGCACCGAGTCATCCTGCCGGACGACGTGCGTGACTTCATCGACAACCTGGACAGA
H V P V C V L G N Y R D M G E H R V I L P D D V R D F I D N L D R

CCTCCAGGTTCCTCCTACTTCCGCTATGCTGAGTCTTCCATGAAGAACAGCTTCGGCCTAAAGTACCTTCATAAGTTCTTCAATATCCCATTTTTGCAGC
P P G S S Y F R Y A E S S M K N S F G L K Y L H K F F N I P F L Q

TTCAGAAGGATGTCAGGCTTGCCCAGGAAAGGGGCTGTGCTGTCGTCCTGGTGTCAGAAGAAGTGAGGATGCCTGCAGGCTGGGACTGCTGCTGGGGACG
L Q K D V R L A Q E R G C A V V L V S E E V R M P A G W D C C W G R

TTTGGGTTGGAAGGAAGGCGGCAGTCAGACTTGTCCTGTGCCGGCACTGCTGGGGAGGCCCCTCCTTCCTGCAGAGCCGTCCCCTCATCACTGGGTTGAT
L G W K E G G S Q T C P V P A L L G R P L L P A E P S P H H W V D

TACTCCTTAGAGAGCTCCCCACTGCTCAGCTGCTCCATTCCCTAA
Y S L E S S P L L S C S I P
```

D. RBEL1D

```
ATGTTTTCCGCCCTGAAGAAGCTGGTGGGGTCGGACCAGGCCCCGGGCCGGGACAAGAACATCCCCGCCGGGCTGCAGTCCATGAACCAGGCGTTGCAGA
M F S A L K K L V G S D Q A P G R D K N I P A G L Q S M N Q A L Q

GGCGCTTCGCCAAGGGGGTGCAGTACAACATGAAGATAGTGATCCGGGGAGACAGGAACACGGGCAAGACAGCGCTGTGGCACCGCCTGCAGGGCCGGCC
R R F A K G V Q Y N M K I V I R G D R N T G K T A L W H R L Q G R P

GTTCGTGGAGGAGTACATCCCCACACAGGAGATCCAGGTCACCAGCATCCACTGGAGCTACAAGACCACGGATGACATCGTGAAGGTTGAAGTCTGGGAT
F V E E Y I P T Q E I Q V T S I H W S Y K T T D D I V K V E V W D

GTAGTAGACAAAGGAAAATGCAAAAAGCGAGGCGACGGCTTAAAGATGGAGAACGACCCCCAGGAGGCGGAGTCTGAAATGGCCCTGGATGCTGAGTTCC
V V D K G K C K K R G D G L K M E N D P Q E A E S E M A L D A E F

TGGACGTGTACAAGAACTGCAACGGGGTGGTCATGATGTTCGACATTACCAAGCAGTGGACCTTCAATTACATTCTCCGGGAGCTTCCAAAAGTGCCCAC
L D V Y K N C N G V V M M F D I T K Q W T F N Y I L R E L P K V P T

CCACGTGCCAGTGTGCGTGCTGGGAACTACCGGGACATGGGCGAGCACCGAGTCATCCTGCCGGACGACGTGCGTGACTTCATCGACAACCTGGACAGA
H V P V C V L G N Y R D M G E H R V I L P D D V R D F I D N L D R

CCTCCAGGTTCCTCCTACTTCCGCTATGCTGAGTCTTCCATGAAGAACAGCTTCGGCCTAAAGTACCTTCATAAGTTCTTCAATATCCCATTTTTGCAGC
P P G S S Y F R Y A E S S M K N S F G L K Y L H K F F N I P F L Q

TTCAGGTAAGCACTCACCACGTGGGGTGGAGTGGCTGCTGGTCTCTCACCTCCTTCCAGGTGTCTCCTGTGTAG
L Q V S T H H V G W S G C W S L T S F Q V S P V
```

mine the expression of the RBEL1C and -D isoforms, we performed Northern blot analysis on a membrane containing total RNAs extracted from a number of cell lines, including MCF-7, T47D, MDA468, MDA231, and Hs578T breast cancer cells and MCF10A normal breast cells. Using an RBEL1 cDNA-specific probe (pan RBEL1 probe, designated as *probe 1* in Fig. 1*A*), that was expected to detect all RBEL1A-D isoforms, we detected a dominant band corresponding to the RBEL1A transcript of ~3.6 kb, which is consistent with our previous findings (22) (Fig. 2*A*, *upper panel*); with prolonged exposure, a band of ~1.6 kb was also revealed (Fig. 2*A*, *middle panel*, *lower arrow*). This low abundant 1.6-kb transcript is expected to represent the RBEL1C mRNA, which has a minimum size of 1563 bp (accession no. GQ169126). However, the RBEL1D mRNA on the same Northern membrane with the pan RBEL1 probe could not be detected (Fig. 2*A*), which could be due to the reasons that (i) RBEL1D transcript is of low abundance and (ii) owing to its predicted size (~3.0 kb), may co-migrate with the highly abundant RBEL1A transcript of 3.8 kb. To further confirm that the ~1.6-kb transcript detected by pan probe was indeed RBEL1C and to determine whether RBEL1D expression was detectable in these cells, we performed additional Northern blot analyses using probes specific only to RBEL1D (Fig. 1*A*, *probe 3*) or to both RBEL1C and -D variants (*probe 2*). As shown in Fig. 2*B*, RBEL1D mRNA expression was detected as a single band of ~3 kb in size when the RBEL1D-specific probe was used, and both the RBEL1C (1.6 kb) and RBEL1D (~3.0 kb) transcripts were weakly detected when a probe specific to both of these isoforms was utilized (Fig. 2*C*). The mRNA expression of both RBEL1C and RBEL1D was also examined by RT-PCR in MCF-7 breast cancer cells, and we detected full-length RBEL1C and RBEL1D cDNAs (confirmed by DNA sequencing) using this approach (data not shown). Thus, our data suggest that RBEL1D and C mRNAs are expressed in these cells albeit at levels lower than those of RBEL1A.

Next, we used the RBEL1 antibody generated in our laboratory (22) to analyze RBEL1C and -D protein expression. The RBEL1 antibody was raised against a peptide corresponding to the RBEL1 N-terminal sequence that is shared by all isoforms. To assess the specific migration pattern of the RBEL1 isoforms, we also employed the lentiviral-mediated RBEL1 shRNA knockdown approach in combination with Western blot analysis. For knockdown purposes, we designed RBEL1 shRNA #59 and #60 to target all RBEL1 isoforms, whereas RBEL1 shRNA #58 was designed to affect only A and B variants. The RBEL1 shRNA #61 and #62 were specific only to the A isoform. Anti-RBEL1 Western blot analyses shown in Fig. 3, *A* and *B*, indicate that, while the control scrambled shRNA had no effect on the expression of the RBEL1 isoforms, the RBEL1-specific shRNAs #58 to #62 specifically knocked down endogenous RBEL1A expression in both MCF-7 and RKO cells (Fig. 3*A*, *top panels*, *lanes 2*, *3*, *5*, and *6*; Fig. 3*B*, *top panels*, *lanes 2–6*, *8*, and *9*). These are expected results, because all of these shRNAs target RBEL1A (shRNAs #58 to #62 targeted regions are depicted in Fig. 1*A*). Anti-RBEL1 Western blotting also detected RBEL1C and RBEL1D protein bands (~40 kDa and ~30 kDa, respectively) when films were exposed for longer time; the size of these two isoforms were very close to their predicted molecular masses (35 kDa for RBEL1C and 28 kDa for RBEL1D). As expected, the levels of both of these proteins were significantly reduced by RBEL1 shRNAs #59 and #60 (which target all RBEL1 isoforms) but not by the RBEL1 shRNAs #58, #61, and #62 (specific for isoform A and/or B) thus, confirming the identities of the RBEL1 isoforms (Fig. 3*B* and data not shown). Fig. 3*C* shows protein expression of RBEL1A, -C, and -D isoforms in several breast cancer cells (MCF-7, T47D, MDA231, and MDA468) and normal breast cells (MCF10A). As shown, RBEL1A protein level is relatively higher than the levels of RBEL1C and -D in the same cells. In addition, all three isoforms (RBEL1A, -C, and -D) are expressed at much higher levels in the cancer cells (MCF-7, T47D, MDA231, and MDA468) than in normal breast cells (MCF10A). We have previously shown that RBEL1A is overexpressed in 67% of primary breast cancers (22). Whether RBEL1C and RBEL1D expression also exhibits a similar expression pattern in human cancers is an important issue and merits further investigation.

We have previously demonstrated that RBEL1A is a glycosylated protein, whereas RBEL1B is not (22). We next sought to also determine the glycosylation status of RBEL1C and -D. As shown in Fig. 3*D*, although RBEL1C (~40 kDa) and RBEL1D (~30 kDa) migrated slightly above the predicted sizes (35 and 28 kDa) on the SDS-PAGE, digestion with NAHase, an enzyme that is known to hydrolyze glycan chains, did not alter HA-RBEL1C and HA-RBEL1D protein migration patterns (Fig. 3*D*, *left panel*, compare *lanes 2* and *3*, and *5* and *6*, with *lanes 1* and *4*, respectively). Similar NAHase digestion, however, did significantly change the migration pattern of RBEL1A, a result consistent with our previous observation (22) (Fig. 3*D*, *right panel*, *lane 8* compared with *lane 7*). Thus, these results suggest that RBEL1C and -D, like the RBEL1B isoform, may not be modified by glycans.

RBEL1C and -D are GTP-binding That Harbor GTPase Activity—We have previously shown that RBEL1A and -B contain GTPase motifs and are predominantly GTP-bound (22). Because RBEL1C and -D are identical to RBEL1A and -B at their N-terminal region harboring the GTP-binding domain, next, we performed GTPase assays to determine the GTP-binding potential of the C and D isoforms. Following in-cell labeling with [^{32}P]orthophosphate, HA-vector alone or HA-tagged RBEL1C and -D proteins were immunoprecipitated with anti-HA antibodies and analyzed. The HA-tagged RBEL1A and -B, which were previously demonstrated to be GTP-binding proteins (22), were also assayed in parallel to serve as positive controls. As shown in Fig. 4*A*, the GTP/GDP binding pat-

FIGURE 1. *A*, genomic organization of the RBEL1 splicing variants: RBEL1A, -B, -C, and -D. The single lines (—) indicate Northern blot probe regions; *arrows* indicate primers used for RT-PCR, and the *gray arrows* represent primer sets used to amplify the full-length open reading frames of RBEL1C (*C1*) and RBEL1D (*D1*); *black arrows* represent the primers used for RT-PCR. The *triple lines* indicate regions of RBEL1 targeted by shRNAs. *B*, schematic representation of the protein domains of RBEL1A-D. *C* and *D*, the nucleotide and amino acid sequences of RBEL1C and RBEL1D. The conserved GTP-binding motifs are *underlined*. The potential CAA*X* motif of RBEL1C is *boxed* and *shaded*.

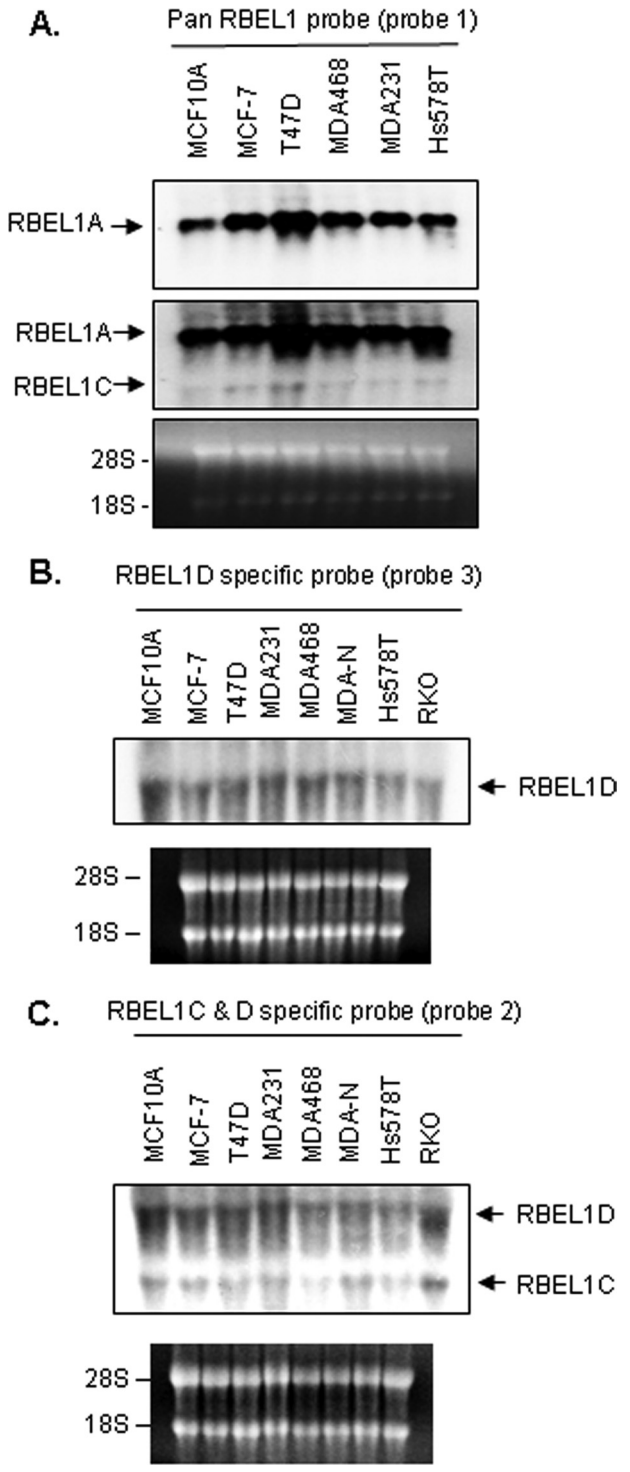

FIGURE 2. *A*, Northern blot analyses of *RBEL1* gene expression in various established cell lines representing normal breast cells (MCF10A) and breast cancer cells (MCF-7, T47D, MDA468, MDA231, and Hs578T). The Northern membrane was probed with a pan RBEL1 probe (Fig. 1*A*, *probe 1*) and exposed for short (*top panel*) and long (*middle panel*) periods of time. *B* and *C*, parallel Northern blot analyses of RBEL1C and -D in various established cell lines representing normal breast cells (MCF10A), breast cancer cells (MCF-7, T47D, MDA231, MDA468, MDA-N-NCI, and Hs578T) and a colon cancer cell line (RKO). In *B*, the Northern membrane was probed with a cDNA probe specific for RBEL1D (Fig. 1*A*, *probe 3*); in *C*, the Northern membrane was probed with a cDNA probed designed to recognize both RBEL1C and RBEL1D (Fig. 1*A*, *probe 2*). Ethidium bromide staining (*lower panels*) depicts RNA loading and integrity.

terns of RBEL1C and -D were clearly different from that of the RBEL1A and -B isoforms. Unlike their RBEL1A and -B counterparts that were mainly GTP-bound, both RBEL1C and RBEL1D were predominantly bound to GDP with a smaller portion of the proteins remaining GTP-bound. Although the functional significance of GTP-GDP binding of these proteins in cellular processes remains to be determined, these results demonstrate that RBEL1C and -D possess active GTPase activity (or active GTPase-activating proteins) and may convert GTP to GDP with faster rate than the RBEL1A and -B isoforms.

RBEL1A and -B Contain an Important GTPase Regulatory Domain within Amino Acid Region 236–302—We analyzed the amino acid sequences of all RBEL1 isoforms to define a region (domain) that was responsible for determining the GTP/GDP-binding potential of the RBEL1 isoforms. Because all of the RBEL1 isoforms share identical N-terminal GTPase domains (encoded by exons 1–6), but differ at their C termini, it was possible that the differences observed in GTP/GDP binding were due to their variable C termini. RBEL1A and -B have relatively longer C-terminal sequences and both are predominantly GTP-bound. RBEL1C and -D, on other hand, have rather short sequences at their C termini. For example, RBEL1D contains only 22 more amino acid residues downstream to the shared GTP-binding domain, and this region also differs between the C and D isoforms, albeit both of these isoforms are predominantly GDP-bound. Based on this information, we speculated that the region(s) that determine(s) the GTP/GDP-binding potential of RBEL1A and -B isoforms could be located within the sequences shared by the A and B isoforms. We further speculated that such a region would likely reside immediately downstream to the GTPase domain in the one or more regions that are identical between RBEL1A and -B. To delineate the mechanisms involving the regulation of GTP/GDP-binding of the RBEL1 proteins, we performed serial deletions of RBEL1A to map the region involved in the regulation of GTP/GDP binding. The deletion variants depicted in Fig. 4*B* show the deletions of potential functional domains of RBEL1A, including the nuclear localization signals, the proline-rich region, and the sequence between these regions. GTPase assays were then performed to determine GTPase activity of these deletion variants. As shown in Fig. 4 (*C* and *D*), all RBEL1A variants with deleted amino acids between 302 and 729 remained dominantly GTP-bound as seen with the full-length RBEL1A; however, deletion involving residues 236–302 (66 amino acids) changed this property, because this variant became primarily GDP-bound (Fig. 4*D*, *lane 3*). Thus, these results suggest that the region containing residues 236–302 in RBEL1A and also in RBEL1B is a potential GTP/GDP-binding regulatory domain, which appears to play an important role in regulating the GTPase activity of RBEL1A and RBEL1B.

The Nucleocytoplasmic Localization of RBEL1C and -D—To determine the subcellular localization of RBEL1C and -D, we tagged both isoforms with HA tags in a mammalian expression vector and analyzed their expression in MCF-7 (breast cancer) and RKO (colon cancer) cells. The anti-HA immunofluorescent staining results presented in Fig. 5 (*A* and *B*) show that,

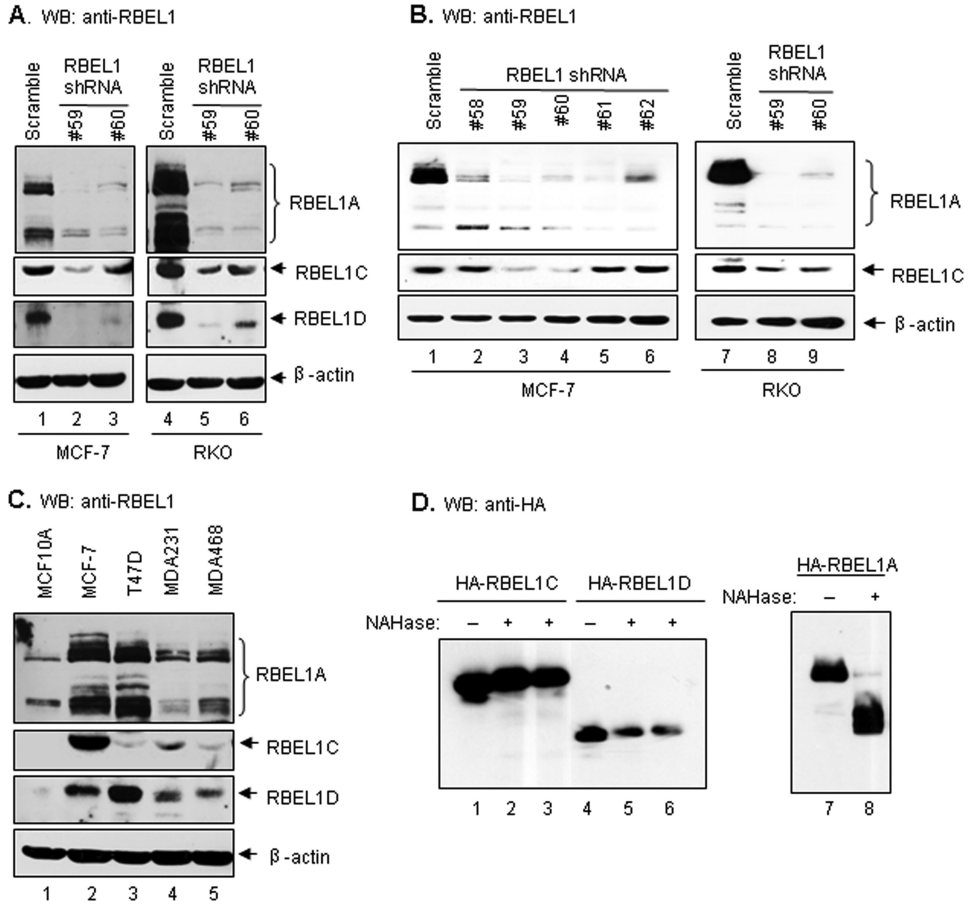

FIGURE 3. *A*, Western blots showing expression of endogenous RBEL1A, -C, and -D in MCF-7 (*left panel*, *lanes 1–3*) and RKO (*right panel*, *lanes 4–6*) cell lines with RBEL1-specific shRNA knockdown (*lanes 2–3* and *5–6*) to indicate specificity of the bands detected by the anti-RBEL1 antibody. *B*, Western blots show RBEL1 shRNA specificity as RBEL1C expression is reduced by shRNAs # 59 and 60, which target all of the RBEL1 splice variants. RBEL1C expression is not affected by RBEL1A specific shRNAs #58, #61, and #62; as expected, all RBEL1 shRNAs reduced the expression of RBEL1A. *C*, Western blots showing relative expression of RBEL1 isoforms in normal breast (MCF10A, *lane 1*) and breast cancer cell lines (MCF-7, T47D, MDA231, and MDA468, *lanes 2–5*). It is of note that, although all three isoforms (A, C, and D) can be detected on the same films, the images for RBEL1C and RBEL1D were obtained with longer exposure (due to low abundant expression) to compare the expression levels of these two proteins in normal and tumor cells. *D*, RBEL1A is the only isoform that is modified by glycans. Western blot analysis showing exogenous HA-RBEL1C (*lanes 1–3*), HA-RBEL1D (*lanes 4–6*), and HA-RBEL1A (*lanes 7–8*) expressed in HEK 293T cells and detected by anti-HA antibodies before (*lanes 1*, *4*, and *7*) or after (*lanes 2*, *3*, *5*, and *8*) treatment with NAHase.

characteristic shared by only a few Ras superfamily GTPases, such as Ran, Rac1, and Rap1 (28–30).

Membrane Binding Potential of the RBEL1 Proteins—Ras superfamily proteins are known to associate with various cellular membranes, including the plasma membrane and membranes of various organelles (1–4). Next, we sought to determine the membrane association of the RBEL1 proteins. HA-empty vector or HA-tagged RBEL1A, -B, -C, and -D expression vectors were transfected into RKO cells and cellular fractionation and sodium carbonate extraction assays were performed. As shown in Fig. 6*A*, a significant portion of all four RBEL1 isoforms (A, B, C, and D) were found to co-segregate with α-tubulin in the supernatant fraction (Fig. 6*A*, *lanes 2* and *3*; Fig. 6*B*, *lanes 2* and *3*), indicating a portion of these proteins reside in the cytosol. In addition, a significant fraction of all four RBEL1 proteins was also found to co-segregate with p97 in the membrane faction (Fig. 6*A*, *lanes 5* and *6*; Fig. 6*B*, *lanes 6* and *7*), indicating that a portion of RBEL1 proteins is associated with membrane. Interestingly, we found that only the higher molecular mass form (~125 kDa) of RBEL1A, but not the lower molecular mass form (~100–110 kDa), could be detected in the membrane fraction (Fig. 6*A*, compare *lane 2* to *lane 5*). The higher molecular mass form of RBEL1A is the glycosylated version of RBEL1A (Fig. 3*D*), and thus, these results suggest that the glycosyl modification may play a role in distribution of RBEL1A to the membrane. In addition, we also found that a fraction of RBEL1B, -C, and -D isoforms (but not the RBEL1A isoform) resisted the membrane extraction with sodium carbonate (100 mM Na_2CO_3, pH 11.5) and co-segregated with the transmembrane protein calnexin (Fig. 6*A*, *lane 9* and Fig. 6*B*, *lanes 10* and *11*). Such results would suggest that at least a part of RBEL1B, RBEL1C, and RBEL1D (but not RBEL1A) might insert into the membranes and tightly associate with the membranes. The RBEL1D active mutant (RBEL1D-R52V) exhibited cellular distribution patterns very similar to that of the wild-type counterpart (RBEL1D-WT) (Fig. 6*B*, *lanes 4*, *8*, and *12*). The differential cellular distribution patterns of the RBEL1 family GTPases would suggest that these proteins may function to differentially regulate cellular processes. Further

although HA alone exhibits only the background staining (Fig. 5, *A* and *B*, *panels e* and *e″*), HA-tagged RBEL1C and -D expression pattern was largely similar to each other, which was distributed in the nucleus as well as in the cytosol (Fig. 5, *A* and *B*, *panels c-c″* and *d-d″*). This expression pattern was rather different from that of RBEL1A and RBEL1B, which was either predominantly cytosolic (for RBEL1A) or primarily nuclear (for RBEL1B) (Fig. 5, *A* and *B*, *panels a-a″* and *b-b″*, and Ref. 22). We also performed cell fractionation assays to determine the distribution of RBEL1C and -D isoforms. Results shown in Fig. 5 (*C* and *D*) indicate that both of these RBEL1 isoforms were localized in the cytosol as well as in the nucleus with a higher portion of the proteins seen in the cytosol. The same blots were probed for lamin B (nuclear) and α-tubulin or β-actin (cytoplasmic) to evaluate the purity of the fractions (Fig. 5, *C* and *D*). Together these results further indicate that the RBEL1 family of GTPases exhibit unique nucleocytoplasmic distribution patterns, a

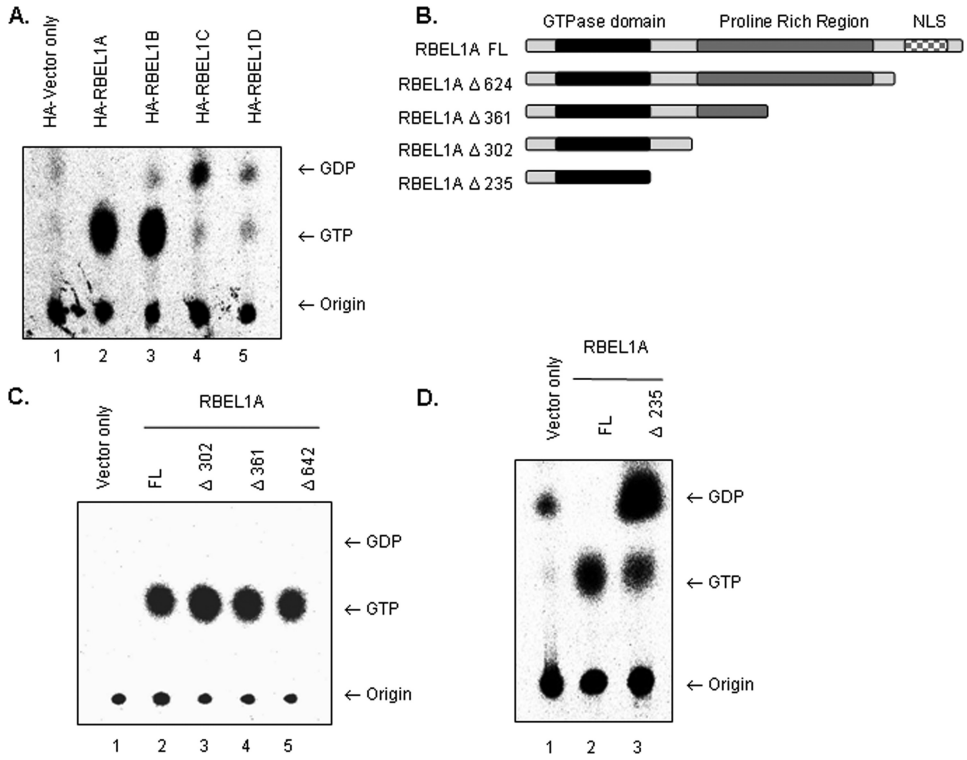

FIGURE 4. *A*, GTP/GDP binding properties of the RBEL1 isoforms. HA tag vector only (*lane 1*) serves as a negative control for background levels nucleotide binding. The GTP/GDP binding assays for HA-tagged RBEL1A (*lane 2*), RBEL1B (*lane 3*), RBEL1C (*lane 4*), and RBEL1D (*lane 5*) were performed as described under "Experimental Procedures." *Arrows* indicate migration of GTP or GDP; the *bottom arrow* points to the origin of samples. *B*, schematic diagram of truncation constructs used in the GTPase assays in panels *C* and *D*. Truncations of the C terminus of full-length RBEL1A (RBEL1A FL) are as follows: RBEL1A Δ624 truncates RBEL1A at amino acid 624. The RBEL1A truncation at amino acid 361 (RBEL1A Δ361) eliminates half of RBEL1A's proline-rich region. The resulting protein product encodes the region of RBEL1A that is identical to RBEL1B. Truncation at amino acid 302 (RBEL1A Δ302) eliminates the rest of the proline-rich region. The deletion construct, RBEL1A Δ235, encodes the N-terminal core GTPase domain that is identical among all the isoforms. *C*, GTPase assays comparing the GTP/GDP-binding potential of full-length HA-RBEL1A (*lane 2*), RBEL1A Δ302 (*lane 3*), RBEL1A Δ361 (*lane 4*), and RBEL1A Δ624 (*lane 5*). Immunoprecipitation of HA-vector only (*lane 1*) served as a negative control. *D*, GTPase assays of the core GTPase domain of RBEL1 (RBEL1A Δ235, *lane 3*) and full-length RBEL1A (*lane 2*); HA-tag vector only (*lane 1*) serves as a negative control for background levels GTP and GDP.

studies are needed and in progress to delineate the functions of these novel GTPases.

RBEL1 Knockdown Results in Cell Growth Suppression and Apoptosis—To gain insight into the potential function of RBEL1 proteins, we used a lentiviral shRNA-mediated knockdown approach (31) to suppress the expression of endogenous RBEL1 and to determine the effect of RBEL1 expression in cell growth. In this regard, we designed five different RBEL1-specific shRNAs that target different regions of RBEL1A (Fig. 1*A*), and suppression of RBEL1 variants by the RBEL1 shRNAs was confirmed (Fig. 7*A* and Fig. 3, *A* and *B*). We used this approach to ensure that the RBEL1 RNA interference did not generate off-target effects. We then determined the effect of RBEL1 shRNAs on tumor cell growth/proliferation. Results of MTT-based cell proliferation assays and cell doubling time assays shown in Fig. 7 demonstrate that expression of all five RBEL1 shRNAs strongly suppressed cell proliferation in the MCF7 breast cancer cell line (Fig. 7, *B* and *E*) and RKO colon cancer cell line (Fig. 7*C*). Fig. 7*D* shows a representative photomicrograph of MCF-7 and RKO cells infected with lentiviral scrambled shRNA (*panel 1*) or three different RBEL1-specific shRNAs (#58, #60, and #62; *panels 2–4*). As is shown, suppression of RBEL1 expression not only caused a significant reduction in cell number in RBEL1 shRNA-expressing cells but also altered cellular morphological appearance. For example, in the RBEL1 shRNA-expressing cells some became spindle-like, and more cells were rounded up and detached from the tissue culture plates, a characteristic of cell death. Because RBEL1A is the most abundant transcript among the various RBEL1 isoforms and is highly expressed in many cancer cell lines, we next sought to determine whether knockdown of RBEL1A alone could attribute to cell growth suppression. MCF-7 cells were infected with the lentiviral scrambled shRNA or shRNAs specific to RBEL1A alone (#61 and #62) or specific to both A and B isoforms (#58). As shown in Fig. 7 (*E* and *B*), knockdown of RBEL1A alone by shRNAs #61, #62, and #58 similarly caused severe cell growth suppression. These results suggest that knockdown of RBEL1A alone could have detrimental effect on cell growth/survival. Next, we re-introduced an RBEL1A cDNA expression vector into MCF-7 RBEL1 knockdown cells infected with lentiviral RBEL1 shRNA #58 to see if re-introduction of RBEL1A protein could reverse the growth suppressive effect of endogenous RBEL1 knockdown. It is of note that shRNA #58 is only specific to the RBEL1A and -B isoforms, and the nucleotide target sequence of shRNA #58 is not located within the coding region of the *RBEL1* gene; thus it would not affect the expression of the exogenous RBEL1A cDNA in the expression vector that lacks sequence corresponding to shRNA #58. As shown in Fig. 7*F*, the growth suppression mediated by RBEL1 shRNA#58 in MCF-7 cells was rescued by the expression of exogenous RBEL1A expression vector. Together these results suggest that RBEL1A expression is linked to maintaining cell growth and survival.

RBEL1 knockdown-mediated growth suppression could be due to inhibition of cell proliferation or induction of cell death. Next, we sought to investigate whether *RBEL1* gene knockdown causes cells to undergo apoptosis. To that end, we investigated the morphological and biochemical features of apoptosis in cells with RBEL1 knockdown. Results of nuclear 4′,6-diamidino-2-phenylindole staining shown in Fig. 8*A* indicate that cells expressing the RBEL1 shRNA (but not scrambled shRNA) show typical features of apoptosis such as nuclear condensation and chromatin fragmentation. We then performed caspase-3

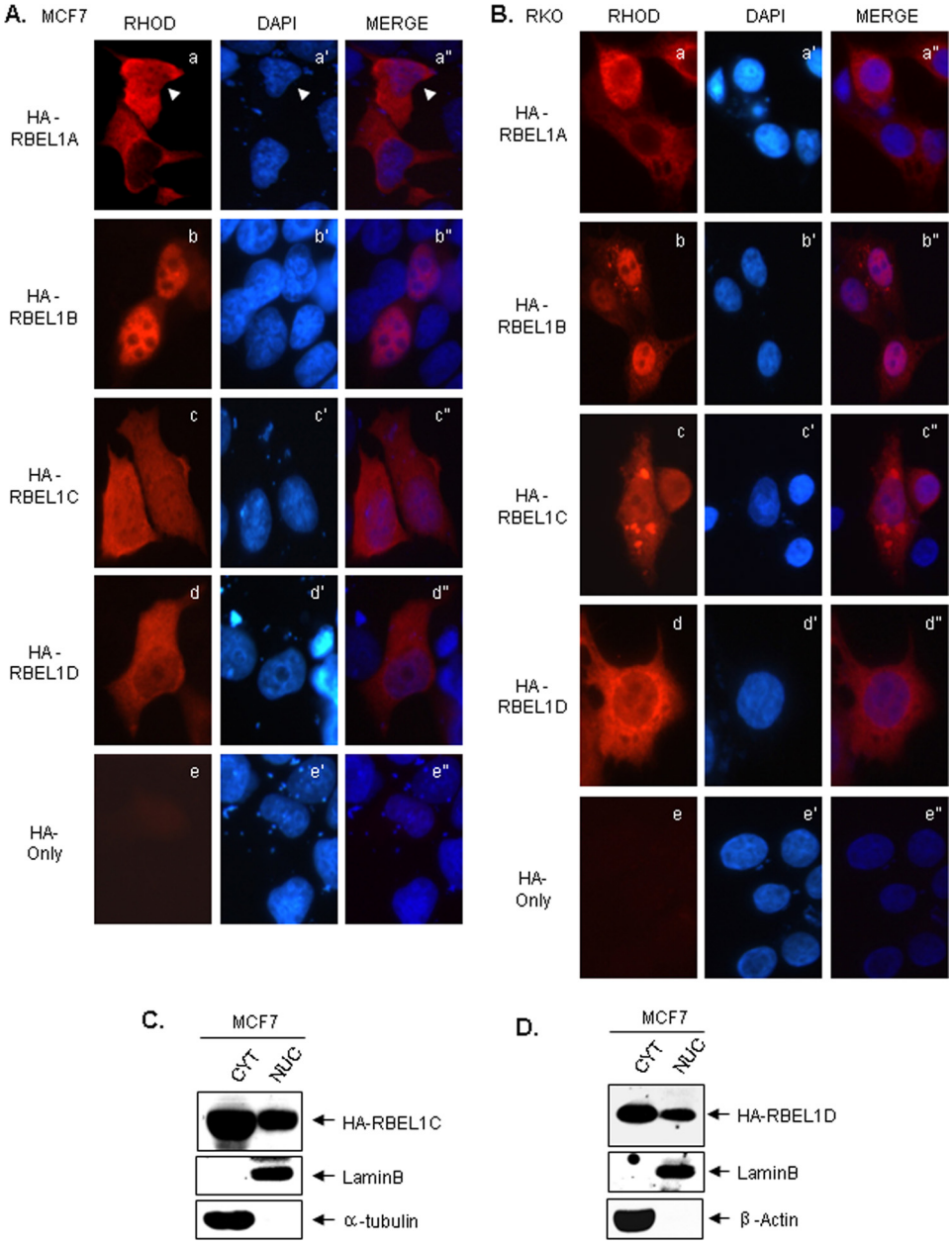

FIGURE 5. *A* and *B*, representative photomicrographs depicting the subcellular distribution of exogenous HA-RBEL1A (*a-a″*), HA-RBEL1B (*b-b″*), HA-RBEL1C (*c-c″*), and HA-RBEL1D (*d-d″*) in MCF-7 (*A*) and RKO (*B*) cells. The HA-tag-only vector was transfected as negative control to assess background and nonspecific fluorescence (*A* and *B*, *e-e″*). *C* and *D*, Western blot analyses of the nuclear and cytoplasmic expression patterns of exogenous HA-RBEL1C (*C*) and HA-RBEL1D (*D*) in MCF-7 cells analyzed by cell fractionation. The cytosolic (*CYT*) and nuclear (*NUC*) fractions were separated as described under "Experimental Procedures." Lamin B served as a protein marker for nuclear fraction purity, and α-tubulin (*C*) or β-actin (*D*) served as protein markers for cytosolic fraction purity.

activity assay, and results shown in Fig. 8*B* demonstrate that RBEL1 knockdown by two different RBEL1 targeting shRNA induce caspase 3 activation. Together these results indicate that RBEL1 knockdown-mediated growth suppression occurs, at least in part, due to the activation of apoptotic signals and suggest that RBEL1 family proteins may play an important role in regulation of cell survival.

RBEL1 Proteins Regulate the ERK Signaling Pathways—We further investigated whether RBEL1 proteins have Ras-like effects in regulation of cellular signal transduction. Extracellular signal-regulated kinase (ERK)-controlled pathway is known to be one of the most important signaling pathways in Ras-mediated regulatory controls modulating cell growth and survival. We, therefore, sought to examine the effect of RBEL1 proteins on ERK and to that end, we first transiently expressed the exogenous RBEL1A, -B, -C, and -D isoforms individually in MCF-7 cells and examined their effects on ERK1/2 phosphorylation. Our results shown in Fig. 9*A* indicate that exogenous expression of all four RBEL1 variants modestly enhanced ERK phosphorylation (especially ERK2), although RBEL1A exhibited more evident effect. Because these experiments involved transient transfections, it is likely that not all cells were transfected by the expression plasmids. Therefore, we also investigated the effect of REBL1 on ERK via the RBEL1 knockdown approach. Our results shown in Fig. 9*B* indicate that RBEL1 knockdown by three different shRNA constructs (#59, #60, and #61) clearly blunted ERK phosphorylation indicating that RBEL1 proteins are important positive regulators of ERK signaling.

DISCUSSION

We have recently reported the identification a novel protein that we named RBEL1. Earlier characterization of RBEL1 had led to the identification of two isoforms named RBEL1A and RBEL1B. Both RBEL1A and RBEL1B were found to exhibit GTP-binding potential, and the mRNA of the predominant isoform, RBEL1A, was found to be overexpressed in the majority of primary human breast cancers (22). Our previous findings suggested RBEL1 to be an important member of the Ras superfamily that could be linked to cell growth regulation, however, additional studies were needed to further characterize RBEL1 and to elucidate its role in cell growth regulation.

In the present study, we have identified and characterized two additional splice variants of the *RBEL1* gene, which we have named RBEL1C and RBEL1D. We have demonstrated that RBEL1C and -D are two new GTPases that bind to both GTP and GDP, although a higher proportion of these proteins is GDP-bound. Our results indicate that all RBEL1 isoforms, including RBEL1A, -B, -C, and -D are identical at their N ter-

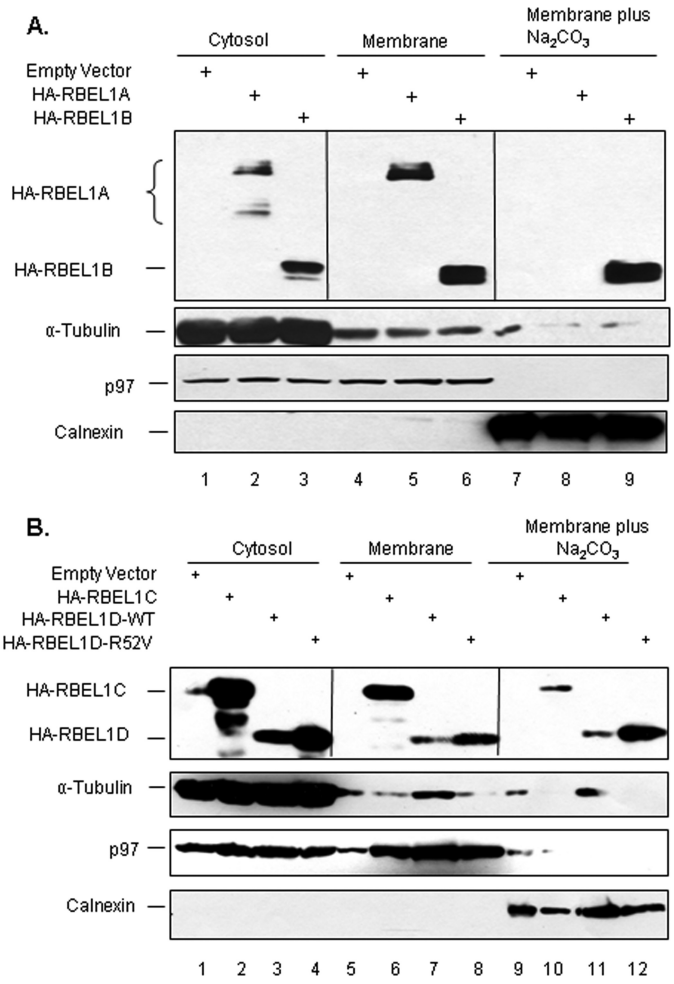

FIGURE 6. **Membrane-binding potential of the RBEL1 proteins.** Membrane fractionation and membrane sodium carbonate extraction assays were performed as described under "Experimental Procedures." RKO cells were transiently transfected with HA-empty vector or HA-tagged RBEL1A, -B, -C, and -D expression vectors. 24 h later, cells were harvested, and cell lysates were subjected to cellular fractionation and sodium carbonate extraction. Protein distribution of the RBEL1A and -B isoforms is shown in *A* and that for RBEL1C and -D isoforms is shown in *B*. It is of note that, in the cytosolic fraction, RBEL1A protein (*lane 2*) has two dominant bands: one is at ~125 kDa (*upper band*, the glycosylated form) and another one is ~100–110 kDa (the non-glycosylated form). In the membrane-associated fraction (*lane 5*), RBEL1A only has one dominant band at ~125 kDa. No RBEL1A band is seen in the sodium carbonate extraction fraction (*lane 8*). It is of note that ~20% of the total volume of each fraction (except for RBEL1D-wild type (*RBEL1D-WT*), which 40% of the total volume was used) was loaded in each lane. α-Tubulin served as a protein marker for cytosolic fraction purity, p97 served as a protein marker for membrane-associated fraction purity, and calnexin served as a protein marker for transmembrane fraction purity.

mini that harbor a GTP-binding domain. The N-terminal GTP-binding domain of RBEL1 isoforms also shares significant amino acid similarity with other Ras superfamily GTPases. It is known that all Ras superfamily proteins are homologous at their N-terminal GTP-binding domains but diverge from each other at their C termini (2, 4). Interestingly, among the Ras superfamily proteins, RBEL1 GTPases share a higher degree of homology to Rab (34–40%), Ran (34%), and Ras (32–36%) subfamily proteins and a lesser degree of homology to Rho/Rac (28–32%), Arf/Sar (28–33%), and G_α (16–19%) subfamilies (Fig. 10). It is of note that RBEL1 proteins do not show similar homology to non-Ras family GTPases such as eEF1A, GBP1, elF5B, and Dynamin suggesting that the RBEL1 GTP-binding proteins belong to the Ras superfamily.

Interestingly, although RBEL1 proteins share homology with five other known subfamily members (Ras, Rho, Rab, Sar1/Arf, and Ran) within the Ras superfamily, they also have a number of unique characteristics that set them apart from these proteins. First, although most of known Ras superfamily proteins are smaller with molecular masses ranging from 20 to 30 kDa (2), RBEL1A and -B isoforms are much larger. For example, RBEL1A is composed of 729 amino acids and has a molecular mass of ~80 to 125 kDa. RBEL1B contains 520 amino acids; its molecular mass ranges from ~62 to ~75 kDa. RBEL1C and RBEL1D, on other hand, are somewhat smaller with molecular masses of ~40 kDa and ~30 kDa, respectively. Second, the RBEL1 proteins exhibit unique subcellular localization. All RBEL1 isoforms are detected in both the nucleus and cytoplasm, albeit there are some differences in their relative nucleocytoplasmic distributions. For example, RBEL1A is predominantly cytosolic even though it contains several putative nuclear localization signals near the end of the C terminus, whereas RBEL1B is primarily nuclear but does not contain obvious nuclear localization signal. RBEL1C and RBEL1D exhibit similar subcellular localizations that are almost evenly distributed between the cytosol and nucleus. It is of note that nuclear localization is a rare occurrence in the Ras superfamily, because only a few members, such as Ran, Rac1, and Rap1, have been found to localize to the nucleus (28–30).

Interestingly, RBEL1 proteins also share some similarity with the Ras superfamily proteins in terms of their membrane association. It is known that most of the Ras superfamily proteins contain the CAA*X* motif at their C termini, and the cysteine residue is mostly prenylated (either farnesylated or geranylgeranylated). Prenylation facilitates these small GTPases to anchor into either the cytoplasmic membrane or membranes of other cellular organelles. Of the four RBEL1 isoforms (A, B, C, and D) characterized in our studies, only the RBEL1C ends with cysteine residue at its C terminus ("CSIP"); RBEL1A, -B, and -D all do not contain the CAA*X* motif expected to be used for protein prenylation. Interestingly, like many other Ras superfamily proteins, all four RBEL1 proteins could be detected to associate with membrane (Fig. 6). In addition, RBEL1B, -C, and -D isoforms resist to membrane extraction with sodium carbonate a finding that suggests membrane association to be important for the RBEL1 protein function.

That RBEL1A is glycosylated is another unique characteristic. As noted above, RBEL1A possess 729 amino acids with a predicted molecular mass of ~80 kDa. On SDS-PAGE analysis, RBEL1A migrates as four major species of ~125, ~110, ~100, and ~80 kDa with the predominant species migrating at the ~125-kDa range. RBEL1A is predicted to harbor multiple glycosylation sites, and de-glycosylation of RBEL1A with NAHase reduces RBEL1A's mass from 125 kDa to around 110 and 100 kDa, indicating that RBEL1A glycosylation is responsible, at least in part, for its larger molecular mass. It is of note that RBEL1A is the only RBEL1 variant to be glycosylated, and it is also the most abundant isoform. Thus, glycosylation of RBEL1A is a unique feature that has not been reported for any other Ras superfamily protein. Importantly, our results indicate

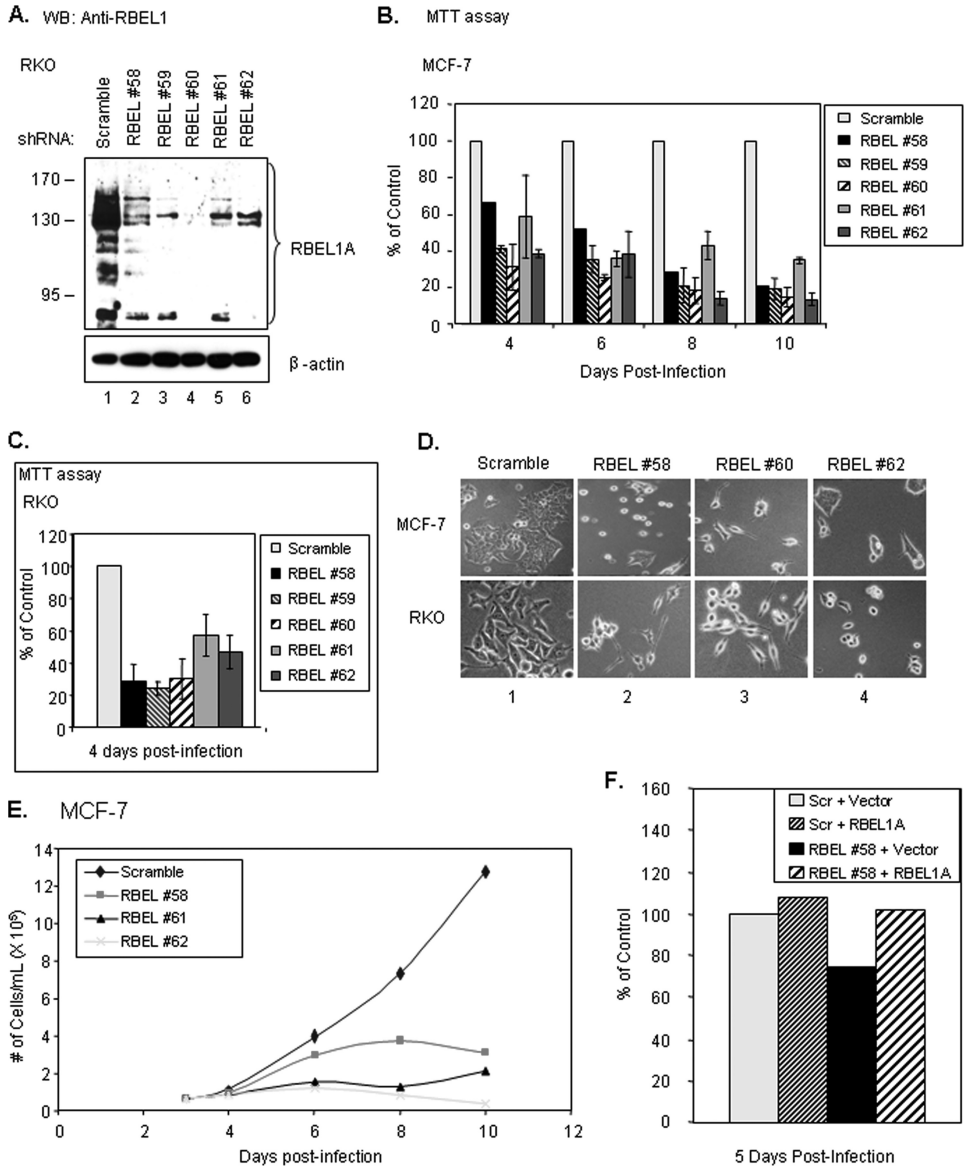

FIGURE 7. **The effect of RBEL1 knockdown on RBEL1A expression and tumor cell growth.** *A*, Western blot analyses using anti-RBEL1 antibody demonstrates suppression of endogenous RBEL1A expression by lentiviral-based knockdown in RKO cells. *Lane 1*, scrambled control shRNA; *lanes 2–6*, five different RBEL1-specific shRNAs designed to target different sequences (*regions* depicted in Fig. 1*C*) of the *RBEL1* gene. *B*, graphic representation of MTT assays depicting decreased cell proliferation due to RBEL1 knockdown in MCF-7 cells. Infected (m.o.i. = 0.3) MCF-7 cells were plated at equal density 3 days post-infection, and MTT assays were performed 4, 6, 8, and 10 days post-infection. Values represent the means ± S.E. of two independent experiments (except shRNA #58, which was studied in only one experiment). *C*, graphic representation of MTT assays in RKO cells infected (m.o.i. = 0.3) with all five RBEL1 shRNAs and scrambled control. Assays were performed as in *B*, except MTT assays were all done 4 days post-infection. Values represent the means ± S.E. of two independent experiments. *D*, representative photomicrographs of cell morphology and growth suppression in cells infected (m.o.i. = 0.3) with RBEL1 shRNAs (RBEL1 #58, #60, and #62) or scrambled shRNA, 10 days post-infection in MCF-7 (*top panels*) and RKO (*bottom panels*) cells. *E*, growth curves of MCF-7 cells infected with the lentiviral particles (m.o.i. = 0.3) bearing the control scrambled shRNA (◆) or three different RBEL1 shRNAs (#58, ■; #61, ▲; and #62, **X**). Equal numbers of cells were plated in 60-mm plates 3 days post-infection, and trypan-blue-excluded cells were counted under a light microscope on days 4, 6, 8, and 10 post-infection. *F*, expression of RBEL1A cDNA prior to shRNA infection protects MCF-7 cells from RBEL1A knockdown-mediated growth suppression. MCF-7 cells were transfected for 6 h with either vector control or RBEL1A expression constructs. Cells were allowed to recover for a few hours, then were infected (m.o.i. = 0.3) with either scrambled or RBEL1 #58 shRNAs overnight. MTT assays were performed 5 days post-infection.

that glycosylation appears to regulate RBEL1A cellular distribution, because we found that only the glycosylated version of RBEL1A associates with membrane (Fig. 6*A*), whereas the non-glycosylated version does not. These results suggest that glycosyl modification may facilitate RBEL1A membrane association, and it will be important to investigate the molecular mechanisms involving such regulation.

Information generated from our studies suggests that, although RBEL1 proteins belong to the Ras superfamily, they do not appear to fit into any of the existing subfamilies in the Ras superfamily. Based on the amino acid comparison, RBEL1 proteins exhibit more homology (34–40% at their N termini) to Rab subfamily of proteins, but RBEL1 proteins do not appear to belong to this subfamily. For example, at their N-terminal GTP-binding domain, Rab GTPases share ~50–70% homology with one another, whereas RBEL1 shares only 34–40% homology to Rab subfamily members. In addition, the GTP-binding motifs of the RBEL1 proteins also deviate from the canonical consensus sequences of the Rab subfamily protein in the third (D*XX*G (K/Q)→D*XX**D***K), fourth (NK*X*D→N***Y****X*D), and fifth (E*X*SA*X*→E*XS**M**X*) GTP-binding motifs. Furthermore, RBEL1 also deviates significantly from Rab subfamily-specific sequences in and around the GTP-binding motifs (*boxed* in Fig 10). Interestingly, RBEL1 proteins also share significant homology (34%) with Ran protein at their N termini. Ran is mostly placed within a subfamily of its own (4, 6, 32) but is also considered by some as a Rab-like protein (2). Ran distributes in the nucleus as well as in the cytosol, and it is an important regulatory protein for facilitating protein transport across the nuclear membrane pore (6, 32). All RBEL1 proteins we have studied also exhibit a nucleocytoplasmic distribution pattern, a characteristic noted less frequently for the Ras superfamily members but displayed by the Ran protein. Rab proteins, on other hand, are all found to reside only in the cytosol but not in the nucleus (8, 9, 11–13). In this context, RBEL1 proteins appear to share some commonalities with Ran. However, RBEL1 proteins also possess some other characteristics that do not appear to place them within the Ran subfamily. For example, RBEL1A is much larger (80–125 kDa) than Ran (24 kDa); it predominantly resides in the cytosol

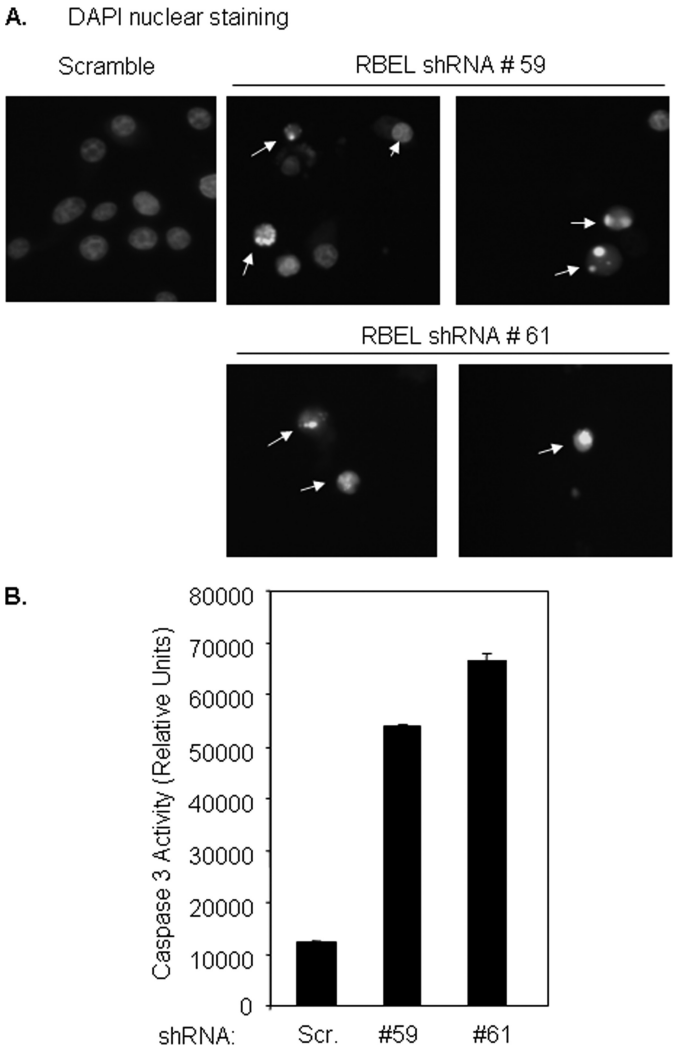

FIGURE 8. **RBEL1 RNA interference knockdown induces apoptosis in MCF7 cells.** A 4′,6-diamidino-2-phenylindole (*DAPI*) nuclear staining assay was performed as we have previously described (23, 25). *Arrows* indicate apoptotic cells. *G*, caspase-3 enzymatic activity in cells expressing the scrambled shRNA or RBEL1 shRNAs (#59 and #61). Caspase-3 enzymatic activity assays were performed as described under "Experimental Procedures."

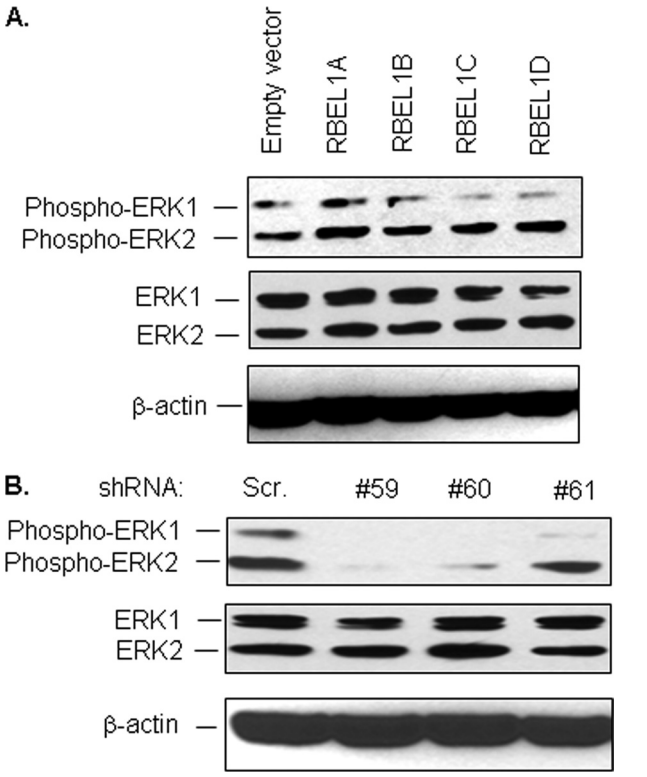

FIGURE 9. **The effect of RBEL1 proteins on ERK phosphorylation.** *A*, MCF-7 cells were transiently transfected with empty vector or HA-tagged RBEL1A, -B, -C, and -D expression constructs. 24 h after transfection, cells were harvested and Western blot analysis was performed using phospho-ERK antibodies, pan-ERK, and β-actin antibodies. *B*, RBEL1 knockdown significantly inhibits ERK phosphorylation. MCF-7 cells were introduced with RBEL1 targeting shRNAs (#59, #60, and #61) as described under "Experimental Procedures." Four days later, cells were harvested and cell lysates were analyzed by Western blotting using ERK phospho-specific antibodies as well as pan-ERK and β-actin antibodies.

although small portion of the protein is also noted in the nucleus; and it is almost exclusively GTP-bound; all of these features are not shared by Ran. Further, Ran itself is significantly more similar to the Rab subfamily proteins (~51% homology) than to RBEL1 proteins (34% homology). Taken together, our findings suggest that RBEL1 proteins appear to belong to a novel subfamily within the Ras superfamily, and Rab and Ran seem to be their close relatives.

Our current studies have also defined a region (domain) in RBEL1A and -B that is important for determining the GTP/GDP-binding potential of the RBEL1 isoforms. Our studies have shown that, although all RBEL1 isoforms share an identical GTP-binding domain, they are very different in terms of GTP/GDP-binding potential. For example, RBEL1A and -B isoforms are predominantly GTP-bound while both RBEL1C and -D bind to both GTP and GDP with higher portion of the proteins GDP-bound. The fact that RBEL1C and -D proteins are mainly GDP-bound could suggest that these two proteins are capable of quickly converting GTP to GDP; this may be due to the active GTPase-activating protein activity that is specific to the RBEL1C and -D isoforms. In addition, using deletion variants we have defined a 66-amino acid region (amino acids 236–302) in RBEL1A and -B that is responsible for these proteins being predominantly GTP-bound. Our studies demonstrate that deletion of the amino acid 236–302 region converts RBEL1A from predominantly GTP-bound to GDP-bound (Fig. 4*D*). It is of note that the region corresponding to residues 236–302 is shared by both RBEL1A and -B but not by RBEL1C and -D isoforms and, interestingly, both RBEL1C and -D are mostly GDP-bound. Our results thus suggest that the region within residues 236–302 in RBEL1A and -B isoforms corresponds to a GTP/GDP binding regulatory domain that plays an important role in regulation of RBEL1 protein nucleotide-binding potential. It is also interesting that our results consistently show that a single amino acid substitution in RBEL1D (R52V, which is equivalent to H-Ras G12V active GTP-bound mutation) significantly increases expression levels of the RBEL1D protein (Fig. 6*B*). The expression levels of wild-type RBEL1D protein are consistently lower than the expression levels of the mutant form. It is possible that the higher levels of mutant RBEL1D may result due to its increased stability. Future studies will be needed to further elucidate whether this mutation is capable of enhancing GTP-binding of the protein and thus increased protein stability and expression.

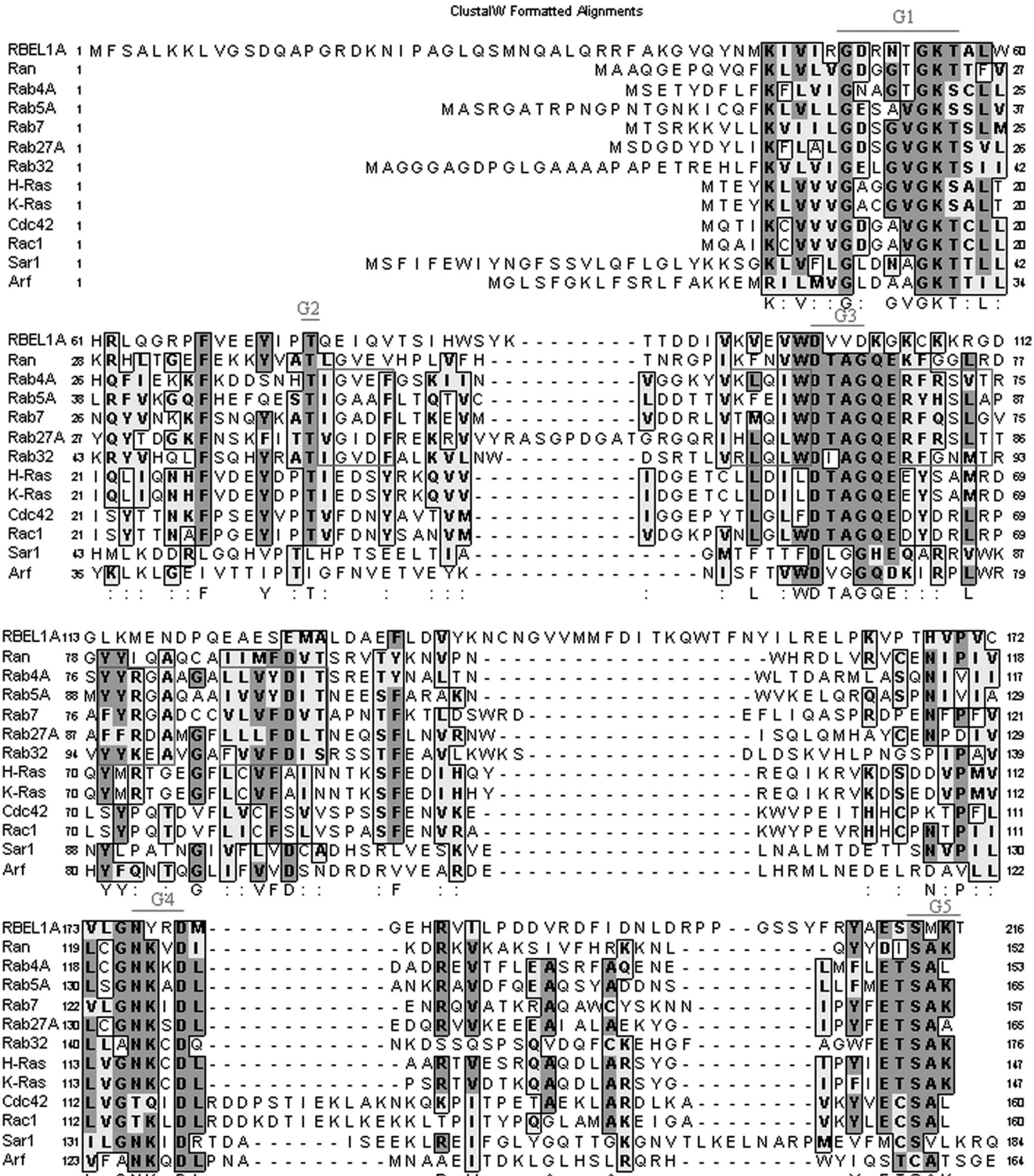

FIGURE 10. **ClustalW alignment of the N terminus of RBEL1 with members of the Ras superfamily generated using MacVector 6.5.3.** *Shaded residues* indicate regions of amino acid homology; the *dark gray areas* indicate identical amino acids and *light gray areas* indicate similar amino acids. The consensus GTP-binding motifs (*G1–G5*) are indicated in *red*. *Areas boxed in red* indicate the Rab subfamily-specific motifs.

Results from our current studies also indicate that RBEL1A plays an important role in cell growth regulation. We have shown that RBEL1 knockdown results in remarkable cell growth suppression associated with apoptosis. Our data further indicate that RBEL1 proteins regulate the ERK signaling pathway. Overexpression of RBEL1 proteins leads to enhanced ERK phosphorylation, and RBEL1 knockdown significantly blunts ERK phosphorylation. Therefore, our studies provide important information that the RBEL1 knockdown-mediated growth suppression and apoptosis may occur, at least in part, due to suppression of ERK signaling. Although the in-depth mechanisms of RBEL1A knockdown-mediated cell growth suppres-

sion and cell death remain to be further elucidated, these results, in conjunction with our previous findings indicating RBEL1A to be overexpressed in many primary human breast cancers, suggest that RBEL1A appears to play an important role in promoting cell growth and/or maintaining cell survival.

In summary, our results provide valuable new information about the identification and characterization of RBEL1 proteins that appear to represent a potentially novel subfamily within the Ras superfamily. Our studies have also provided valuable insight into the function and regulation of these proteins highlighting the regulation of their GTP/GDP-binding potential and their role in modulating cell growth and survival.

REFERENCES

1. Bos, J. L. (1989) *Cancer Res.* **49,** 4682–4689
2. Colicelli, J. (2004) *Sci. STKE 2004,* RE13
3. Konstantinopoulos, P. A., Karamouzis, M. V., and Papavassiliou, A. G. (2007) *Nat. Rev. Drug Discov.* **6,** 541–555
4. Takai, Y., Sasaki, T., and Matozaki, T. (2001) *Physiol. Rev.* **81,** 154–208
5. Rajalingam, K., Schreck, R., Rapp, U. R., and Albert, S. (2007) *Biochim. Biophys. Acta* **1773,** 1177–1195
6. Quimby, B. B., and Dasso, M. (2003) *Curr. Opin. Cell Biol.* **15,** 338–344
7. Ciciarello, M., Mangiacasale, R., and Lavia, P. (2007) *Cell Mol. Life Sci.* **64,** 1891–1914
8. Darchen, F., and Goud, B. (2000) *Biochimie* (*Paris*) **82,** 375–384
9. Deneka, M., Neeft, M., and Van der Sluijs, P. (2003) *Crit. Rev. Biochem. Mol. Biol.* **38,** 121–142
10. Pereira-Leal, J. B., and Seabra, M. C. (2000) *J. Mol. Biol.* **301,** 1077–1087
11. Pfeffer, S. R. (2001) *Trends Cell Biol.* **11,** 487–491
12. Stenmark, H., and Olkkonen, V. M. (2001) *Genome Biology* **2,** 3007.1–3007.7
13. Zerial, M., and McBride, H. (2001) *Nat. Rev. Mol. Cell Biol.* **2,** 107–117
14. Vetter, I. R., and Wittinghofer, A. (1999) *Q. Rev. Biophys.* **32,** 1–56
15. Vetter, I. R., and Wittinghofer, A. (2001) *Science* **294,** 1299–1304
16. Geyer, M., and Wittinghofer, A. (1997) *Curr. Opin. Struct. Biol.* **7,** 786–792
17. Bernards, A. (2003) *Biochim. Biophys. Acta* **1603,** 47–82
18. Bos, J. L., Rehmann, H., and Wittinghofer, A. (2007) *Cell* **129,** 865–877
19. Cheng, K. W., Lahad, J. P., Kuo, W. L., Lapuk, A., Yamada, K., Auersperg, N., Liu, J., Smith-McCune, K., Lu, K. H., Fishman, D., Gray, J. W., and Mills, G. B. (2004) *Nat. Med.* **10,** 1251–1256
20. Yao, R., Wang, Y., Lubet, R. A., and You, M. (2003) *Neoplasia* **5,** 41–52
21. Pei, L., Peng, Y., Yang, Y., Ling, X. B., Van Eyndhoven, W. G., Nguyen, K. C., Rubin, M., Hoey, T., Powers, S., and Li, J. (2002) *Cancer Res.* **62,** 5420–5424
22. Montalbano, J., Jin, W., Sheikh, M. S., and Huang, Y. (2007) *J. Biol. Chem.* **282,** 37640–37649
23. Luo, X., He, Q., Huang, Y., and Sheikh, M. S. (2005) *Cancer Res.* **65,** 10725–10733
24. Luo, X., Huang, Y., and Sheikh, M. S. (2003) *Oncogene* **22,** 7247–7257
25. Rong, R., Jin, W., Zhang, J., Sheikh, M. S., and Huang, Y. (2004) *Oncogene* **23,** 8216–8230
26. Huang, Y., Saez, R., Chao, L., Santos, E., Aaronson, S. A., and Chan, A. M. (1995) *Oncogene* **11,** 1255–1260
27. Resh, M. D. (2006) *Nat. Chem. Biol.* **2,** 584–590
28. Fahrenkrog, B., and Aebi, U. (2003) *Nat. Rev. Mol. Cell Biol.* **4,** 757–766
29. Lanning, C. C., Daddona, J. L., Ruiz-Velasco, R., Shafer, S. H., and Williams, C. L. (2004) *J. Biol. Chem.* **279,** 44197–44210
30. Mitra, R. S., Zhang, Z., Henson, B. S., Kurnit, D. M., Carey, T. E., and D'Silva, N. J. (2003) *Oncogene* **22,** 6243–6256
31. Moffat, J., Grueneberg, D. A., Yang, X., Kim, S. Y., Kloepfer, A. M., Hinkle, G., Piqani, B., Eisenhaure, T. M., Luo, B., Grenier, J. K., Carpenter, A. E., Foo, S. Y., Stewart, S. A., Stockwell, B. R., Hacohen, N., Hahn, W. C., Lander, E. S., Sabatini, D. M., and Root, D. E. (2006) *Cell* **124,** 1283–1298
32. Macara, I. G. (2001) *Microbiol. Mol. Biol. Rev.* **65,** 570–594